NUWC-NPT Technical Report 10,426
14 February 1995

Track Initialization Sensitivity in Clutter

Roy L. Streit
Combat Systems Department

Naval Undersea Warfare Center Division
Newport, Rhode Island

PREFACE

The research described in this report was performed under Task 3 of the Platform Acoustic Warfare Data Fusion Project as part of the Submarine/Surface Ship USW Surveillance Technology Program sponsored by the Technology Directorate of the Office of Naval Research, Program Element 0602314N, ONR Technology Program UN3B, Project Number RJ14Q63, NUWC Job Order No. E67801, NUWC principal investigator M. E. Simard (Code 33A), program director G. C. Connolly (Code 2192). The ONR program manager is D. H. Johnson (ONR 321).

The technical reviewer for this report was M. L. Graham (Code 2214).

Reviewed and Approved: 14 February 1995

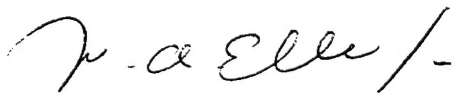

P. A. La Brecque
Head, Combat Systems Department

REPORT DOCUMENTATION PAGE

Form Approved
OMB No. 0704-0188

1. AGENCY USE ONLY *(Leave blank)*	2. REPORT DATE	3. REPORT TYPE AND DATES COVERED
	14 February 1995	Final

4. TITLE AND SUBTITLE

Track Initialization Sensitivity in Clutter

5. FUNDING NUMBERS

6. AUTHOR(S)

Roy L. Streit

7. PERFORMING ORGANIZATION NAME(S) AND ADDRESS(ES)

Naval Undersea Warfare Center Division
1176 Howell Street
Newport, Rhode Island 02841-1708

8. PERFORMING ORGANIZATION REPORT NUMBER

TR 10,426

9. SPONSORING/MONITORING AGENCY NAME(S) AND ADDRESS(ES)

Office of Naval Research
800 North Quincy Street
Arlington, VA 22217-5660

10. SPONSORING/MONITORING AGENCY REPORT NUMBER

11. SUPPLEMENTARY NOTES

12a. DISTRIBUTION/AVAILABILITY STATEMENT

Approved for public release; distribution is unlimited.

12b. DISTRIBUTION CODE

13. ABSTRACT *(Maximum 200 words)*

Sensitivity to track initialization error is quantified as a function of clutter density for the nearest neighbor assignment function (NNAF). Quality of track initialization is thereby related to assignment accuracy. Two statistical distributions of track initialization error are derived under idealized hypotheses representing excellent and poor performance of the NNAF in clutter. A track initialization error region is obtained by constraining the mean initializing error under the excellent NNAF performance hypothesis to have (lower tail) significance level at most α under the poor NNAF performance hypothesis The initialization sensitivity region is derived for general nonlinear state equations and for measurement equations with additive Gaussian noise. Examples using constant velocity models are given.

The methodology is used to define a family of curves called initialization clutter envelope (ICE) curves. ICE curves plot maximum clutter density against maximum initialization error and are useful for estimating the maximum clutter density at which successful tracking can occur for a given initialization error.

There exists a critical clutter density at which the initialization error region is the empty set. Thus, even perfect track initialization is a poor initialization in clutter whose density exceeds critical density. An explicit expression for the critical clutter density is derived.

14. SUBJECT TERMS		15. NUMBER OF PAGES
Target Tracking	Statistical Distribution	23
Tracking Error	Probability Density Function	16. PRICE CODE

17. SECURITY CLASSIFICATION OF REPORT	18. SECURITY CLASSIFICATION OF THIS PAGE	19. SECURITY CLASSIFICATION OF ABSTRACT	20. LIMITATION OF ABSTRACT
Unclassified	Unclassified	Unclassified	SAR

TABLE OF CONTENTS

LIST OF ILLUSTRATIONS

LIST OF TABLES

Reverse Blank

TRACK INITIALIZATION SENSITIVITY IN CLUTTER

1. INTRODUCTION

Track initialization error is quantified as a function of clutter density for the nearest neighbor assignment function (NNAF). Quality of track initialization is thereby related to assignment accuracy. Two statistical distributions of total track initialization error are derived under idealized hypotheses representing excellent and poor performance of the NNAF in clutter. A track initialization sensitivity region is obtained by constraining the mean initialization error under the excellent NNAF performance hypothesis to have (lower tail) significance level at most α under the poor NNAF performance hypothesis. The initialization error region is derived for general nonlinear state equations and for measurement equations with additive Gaussian noise; the initialization error region is not conditioned on particular measurement sets, but it is a function of clutter density and the number of scans in the track initialization. As the number of scans in the initialization increases, examples show that sensitivity to errors in initial velocity increases linearly compared with sensitivity to positional errors when constant velocity models hold.

There exists a critical clutter density at which the initialization error region is the empty set. One interpretation of this result is that even perfect track initialization is a poor initialization in clutter whose density exceeds critical density. The critical clutter density, normalized by the determinant of the additive measurement noise process, depends only on the dimension of the measurement vector; moreover, it is independent of the state and measurement process models. An explicit expression for the critical clutter density is derived.

The methodology is used to define a family of curves called initialization clutter envelop (ICE) curves. ICE curves plot maximum clutter density against maximum initialization error, and they are useful for estimating the maximum clutter density at which successful tracking can occur for a given initialization error. Further details are discussed in section 2.

In practice, measurement assignment functions may use a variety of application-specific "clues" to enhance performance and reduce track estimation error. The problem studied here is restricted to assignment functions that are strictly kinematical. Thus, only the initial target track and the target measurement process are known to the NNAF. Performance limits for the kinematic problem are insightful and useful in themselves, and they facilitate quantitative analysis of the utility of additional clues to the tracking process.

2. INITIALIZATION SENSITIVITY REGION

Precisely one target is assumed present, and an initial track estimate is given. Multiple measurements from a sensor at $T \geq 1$ successive independent scans are available for re-estimating the target track. The probability of detecting the target at each scan is one, so precisely one measurement comes from the target in each scan. Measurements not originating from the target are termed clutter. An automated assignment function selects the measurement corresponding to the target from among the available measurements at each scan. The measurement assigned to the target is presented to the tracking algorithm, and a new estimate of target track is computed.

The assignment function considered here is the NNAF. The NNAF is given a set of (unlabeled) measurements comprising both target and clutter, and the measurement closest to the expected measurement, conditioned on the initial track, is assigned to the target at each scan. The NNAF has the opportunity to commit errors, that is, to select a clutter measurement as the target measurement. An explicit mathematical definition of the NNAF in terms of measurements and initial target track is postponed momentarily (see equation (1)).

A null hypothesis is used to model poor track initialization. The target is always present, by definition, so the null hypothesis cannot be a traditional target absent condition. The null must pertain to the initial track estimate and the strictly kinematic information used by the assignment function. Intuitively, the worst track initializations are so remote from the target track at every scan that the presence of any amount of clutter makes the assignment function fail to select the correct measurement with probability very nearly one. Idealizing this situation leads to the following null hypothesis for poor track initialization:

> $\mathcal{H}$: The NNAF never assigns the correct measurement to the target track; that is, track initialization is such that, at each scan, the measurement assigned to target is a clutter point.

Clutter-induced track estimation error is the only source of estimation error under the null hypothesis $\mathcal{H}$. Intuitively, the likelihood of the NNAF failing completely, as stipulated in hypothesis $\mathcal{H}$, diminishes with decreasing clutter density.

An alternative hypothesis is used to model good track initialization. A simple model is that track initialization is so good that the assignment function is nearly always correct at any clutter density. Idealizing this situation leads to the following alternative hypothesis:

> $\mathcal{K}$: The NNAF is error free; that is, track initialization is such that, at each scan, the measurement assigned to the target is the correct measurement.

Target measurement error is the only source of track estimation error under hypothesis $\mathcal{K}$. Intuitively, the likelihood that the NNAF never makes a wrong assignment, as required by hypothesis $\mathcal{K}$, diminishes with increasing clutter density.

The statistic of interest under $\mathcal{H}$ and $\mathcal{K}$ is a normalized innovation statistic, denoted S, which measures the total squared error (relative to the measurement covariance) of the given track initialization. In sufficiently heavy clutter, the assignment functions modeled by $\mathcal{H}$ and $\mathcal{K}$ are difficult to distinguish using the statistic S. When clutter reaches a certain *critical* density, the nearest neighbor measurement and the target measurement are, on average, equally close to the expected measurement (conditioned on the initial track). Consequently, in clutter of density greater than or equal to critical density, the target track is lost against the noisy background despite the assumption that a target is present. Equating the means of the probability density functions (PDFs) of S under $\mathcal{H}$ and $\mathcal{K}$ gives a fundamental equation relating the clutter density to track initialization and provides a convenient definition of a critical clutter density (see section 3).

Standard approximations to the PDFs of S under $\mathcal{H}$ and $\mathcal{K}$ are derived and used in this report. These approximations are exact under the following modified hypotheses:

$\mathcal{H}'$: The NNAF is given only clutter data, i.e., target is absent.
$\mathcal{K}'$: The NNAF is given only target data, i.e., clutter is absent.

The modified hypotheses are appropriate for detecting target absence or presence. They are adequate approximations for the purposes of studying track initialization sensitivity. Moreover, they provide significant insight into the problem. For these reasons, the hypotheses $\mathcal{H}'$ and $\mathcal{K}'$ are studied in this report. Numerical investigation of track initialization under hypotheses $\mathcal{H}$ and $\mathcal{K}$ will be the subject of a later study.

Distributions for the statistic S under $\mathcal{H}'$ and $\mathcal{K}'$ differ from those under $\mathcal{H}$ and $\mathcal{K}$, a fact that went completely unnoticed in the literature until pointed out in a recent paper by Li.[1] Under hypotheses $\mathcal{H}$ and $\mathcal{K}$, the input to the NNAF comprises unlabeled target and clutter measurements, yet the NNAF does not happen to select incorrect measurements, namely, the target measurement under $\mathcal{H}$ and a clutter measurement under $\mathcal{K}$. Given the opportunity to commit error, hypotheses $\mathcal{H}$ and $\mathcal{K}$ state that no errors occurred. In contrast, under hypotheses $\mathcal{H}'$ and $\mathcal{K}'$, the NNAF cannot select incorrect measurements because the inputs to the NNAF are censored: the target measurement is absent under $\mathcal{H}'$ and clutter measurements are absent under $\mathcal{K}'$.

A track error sensitivity region, denoted by $\mathcal{R}'(\alpha)$, is defined by setting a significance level α for rejecting $\mathcal{H}'$ and requiring the mean of the statistic S under $\mathcal{K}'$ to be significant at this level, i.e., the mean of S under $\mathcal{K}'$ lies on the lower tail of S under $\mathcal{H}'$ at the point of significance α. The defining inequality of the initialization region $\mathcal{R}'(\alpha)$ is derived in this section, as well as receiver operating characteristic (ROC) curves under hypotheses $\mathcal{H}'$ and $\mathcal{K}'$.

A sensor measurement is a vector of $m \geq 1$ real-valued components; that is, each sensor measurement is a point in $\boldsymbol{R}^m$. The normalized distance between two measurements, say z and w, is defined by

$$d(z,w) = \left((z-w)' R^{-1} (z-w)\right)^{\frac{1}{2}}, \tag{1}$$

where, throughout this report, R is the covariance matrix of additive Gaussian measurement noise (see equation (8)). The normalized distance (equation (1)) is used by the NNAF. The sensor's field of view is assumed to comprise all of $\boldsymbol{R}^m$, a simplifying idealization. Clutter is modeled as uniform Poisson (point) clutter over $\boldsymbol{R}^m$ with normalized density parameter $\lambda|R|^{\frac{1}{2}}$, where $|R|$ is the determinant of R. The normalized density is dimensionless; this is a practical advantage for application comparisons. A theoretical justification for the normalized density is as follows: let $R = LL'$, where L is the Cholesky factor of R. Then the transformation $z = Ly$ transforms the normalized distance (equation (1)) into the usual Euclidean distance in $\boldsymbol{R}^m$ and, simultaneously, transforms the Poisson clutter process into another Poisson process with density $\lambda|R|^{\frac{1}{2}}|L^{-1}| = \lambda$. That the density parameter transforms in this way is an immediate consequence of the Mapping Theorem for Poisson processes (see Kingman, section 2.3).[2]

Let $\Omega_m(r)$ denote a normalized sphere in $\boldsymbol{R}^m$ with radius r and centered at any fixed point, say the origin, that is,

$$\Omega_m(r) = \{z \in \boldsymbol{R}^m : d(z,0) \le r\}.$$

The volume of $\Omega_m(r)$ is[3]

$$v_m(r) = \frac{\pi^{\frac{m}{2}} |R|^{\frac{1}{2}} r^m}{\Gamma\left(\frac{m}{2}+1\right)} \equiv \kappa_m |R|^{\frac{1}{2}} r^m. \tag{2}$$

Using properties of the Gamma function and $\Gamma\left(\frac{1}{2}\right) = \pi^{\frac{1}{2}}$ gives the special cases

$$\kappa_1 = 2,\ \kappa_2 = \pi,\ \kappa_3 = \frac{4\pi}{3},\ \textit{and}\ \kappa_4 = \frac{\pi^2}{2}.$$

It is well known[4] that the PDF of the Euclidean distance of the kth closest clutter point to the origin (or any fixed point) is

$$p_k(r) = \frac{m\left(\kappa_m \lambda |R|^{\frac{1}{2}}\right)^k}{(k-1)!} r^{km-1} \exp\left(-\kappa_m \lambda |R|^{\frac{1}{2}} r^m\right).$$

Only the PDF of the closest clutter point is needed in this application, and this is the case $k = 1$; explicitly,

$$p_1(r) = mk_m \lambda |R|^{\frac{1}{2}} r^{m-1} \exp(-\kappa_m \lambda |R|^{\frac{1}{2}} r^m).$$

The PDF of the squared distance of the closest clutter point is, therefore,

$$p(u) \equiv \frac{m}{2} \kappa_m \lambda |R|^{\frac{1}{2}} u^{\frac{m}{2}-1} \exp(-\kappa_m \lambda |R|^{\frac{1}{2}} u^{\frac{m}{2}}), \tag{3}$$

where $u = r^2$. The moments of $p(u)$ are

$$\overline{u^\nu} \equiv \int_0^\infty u^\nu p(u)\, du = \frac{\Gamma(\frac{2\nu}{m}+1)}{(\lambda |R|^{\frac{1}{2}} \kappa_m)^{\frac{2\nu}{m}}} = \frac{\Gamma(\frac{2\nu}{m}+1)}{\pi^\nu} \left[\frac{\Gamma(\frac{m}{2\nu}+1)}{\lambda |R|^{\frac{1}{2}}} \right]^{\frac{2\nu}{m}}, \quad \nu = 0,1,2,\ldots,$$

as is seen via the change of variables $\xi = \kappa_m \lambda |R|^{\frac{1}{2}} u^{\frac{m}{2}}$. In particular,

$$\bar{u} = \frac{\Gamma(\frac{2}{m}+1)}{\pi} \left[\frac{\Gamma(\frac{m}{2}+1)}{\lambda |R|^{\frac{1}{2}}} \right]^{\frac{2}{m}} \tag{4}$$

is the mean-squared distance of the closest clutter point to the origin.

A total of $T \geq 1$ successive independent measurement scans are given. Let r_t denote the normalized distance (equation (1)) of the closest clutter measurement to the origin at time t. Under the null hypothesis $\mathcal{H}'$, the squared distances $u_t = r_t^2$ are independent, so it follows that the total innovation statistic

$$S_{\mathcal{H}'} = \sum_{t=1}^{T} r_t^2 = \sum_{t=1}^{T} u_t, \tag{5}$$

has mean and variance

$$\overline{S_{\mathcal{H}'}} = T\bar{u} \text{ and } var(S_{\mathcal{H}'}) = T^2 \left[\overline{u^2} - (\bar{u})^2 \right]. \tag{6}$$

The statistic $S_{\mathcal{H}'}$ is independent of the target initialization because Poisson clutter is spatially homogeneous in the measurement space, $\boldsymbol{R}^m$. The PDF of the statistic (equation (5)) will be denoted by $p_s(s \mid \kappa_m \lambda |R|^{\frac{1}{2}}, T, \mathcal{H}')$. No explicit form for this PDF is available except for $m = 2$;

however, the appendix shows that useful thresholds for hypothesis testing purposes are readily obtained for all m.

Let $\boldsymbol{R}^n$ denote the target state space. A target initialization comprises a sequence of target states of length T, denoted $X^{initial} = \left(x_1^{initial}, \cdots, x_T^{initial}\right)$, where each state $x_i^{initial} \in \boldsymbol{R}^n$. Position-keeping (PK) track initialization is assumed; i.e.,

$$x_{t+1}^{initial} = F_t(x_t^{initial}),\ t = 1, \ldots, T-1. \tag{7}$$

PK initialization is thus fully characterized by the first point $x_1^{initial}$. Additive Gaussian noise models are assumed for the given nonlinear target measurement process; hence, the target measurement process is modeled by

$$z_t = H_t\left(x_t^{true}\right) + w_t, \tag{8}$$

where the additive noises $\{w_t\}$ are independent and identically distributed with covariance matrix R and $\left\{x_t^{\text{true}}\right\}$ denotes the actual (but unknown) target states. Under hypothesis $\mathcal{H}'$, the correct target measurement is known—only the initialization is erroneous. Hence, the measurement error conditioned on the initialization $X^{initial}$ is given by

$$\begin{aligned}
\varepsilon_t &= z_t - H_t(x_t^{initial}) \\
&= z_t - H_t(x_t^{true}) + H_t(x_t^{true}) - H_t(x_t^{initial}) \\
&= w_t + H_t(x_t^{true}) - H_t(x_t^{initial}).
\end{aligned}$$

The errors $\{\varepsilon_t\}$ are Gaussian distributed with mean vector $H_t\left(x_t^{true}\right) - H_t\left(x_t^{initial}\right)$ and covariance matrix R. The statistic

$$S_{\mathcal{H}'} = \sum_{t=1}^{T} \left(z_t - H_t\left(x_t^{initial}\right)\right)' R^{-1}\left(z_t - H_t\left(x_t^{initial}\right)\right) \tag{9}$$

is distributed $\chi^2_{mT}(\delta) \equiv \chi^2_{mT}(\cdot \mid \delta)$, that is, noncentral chi-squared with mT degrees of freedom and noncentrality parameter

$$\delta = \sum_{t=1}^{T}\left(H_t\left(x_t^{true}\right) - H_t\left(x_t^{initial}\right)\right)' R^{-1}\left(H_t\left(x_t^{true}\right) - H_t\left(x_t^{initial}\right)\right). \tag{10}$$

This result follows easily from Muirhead (Theorems 1.3.4 and 1.4.1).[5] The noncentrality parameter is the total squared initialization error. The mean and variance of $S_{\mathcal{H}'}$ are (see Muirhead, page 24)[5]

$$\overline{S_{\kappa'}} = mT + \delta \text{ and } var(S_{\kappa'}) = 2mT + 4\delta. \tag{11}$$

Because of PK initialization, the statistic $S_{\kappa'}$ is conditioned solely on the first point $x_1^{initial}$ of $X^{initial}$.

If measurement process is linear, so that $H_t(x) = H_t x$ for all x, then the total squared initialization error can be written in the form

$$\delta = \sum_{t=1}^{T} \left(F_t\left(x_t^{true}\right) - F_t\left(x_t^{initial}\right)\right)' \left(H_t\right)' R^{-1} H_t\left(F_t\left(x_t^{true}\right) - F_t\left(x_t^{initial}\right)\right). \tag{12}$$

Further, if the target process is linear, so that $F_t(x) = F_t x$ for all x, then

$$\delta = \Delta' W \Delta,$$

where

$$\Delta = x_1^{true} - x_1^{initial} \tag{13}$$

is the track initialization error vector at time $t = 1$, and the matrix W is given by

$$W = \sum_{t=1}^{T} \left(\prod_{j=0}^{t-1} F_j\right)' \left(H_t\right) R^{-1} H_t \left(\prod_{j=0}^{t-1} F_j\right),$$

where F_0 is the $n \times n$ identity matrix. If the target process is stationary also, so that $F_t(x) = F x$ for all t, then W simplifies further to

$$W = \sum_{t=1}^{T} \left(H_t F^{t-1}\right)' R^{-1} \left(H_t F^{t-1}\right). \tag{14}$$

Further simplification of W seems possible only in special cases. The matrix W is clearly positive semidefinite, as is evident from equation (12). In many practical problems, F and $\{H_t\}$ are such that W is positive definite; however, no general condition for the positive definiteness of W is presented here.

Let the significance level α for rejecting the hypothesis $\mathcal{H}'$ be specified. If the normalized clutter density is such that $\lambda |R|^{\frac{1}{2}} \le \lambda_{critical} |R|^{\frac{1}{2}}$, where $\lambda_{critical}$ is defined in section 3, then the quantity $s_\alpha(\kappa_m \lambda |R|^{\frac{1}{2}}, T)$ satisfying the equation

$$1-\alpha = \int_{s_\alpha(\kappa_m\lambda|R|^{\frac{1}{2}},T)}^{\infty} p_S(\xi \mid \kappa_m\lambda|R|^{\frac{1}{2}}, T, \mathcal{H}')\, d\xi, \tag{15}$$

defines the threshold at significance level α for rejecting $\mathcal{H}'$ in a traditional lower-tail significance test. The threshold $s_\alpha(\kappa_m\lambda|R|^{\frac{1}{2}}, T)$ depends on α, the normalized clutter density, and the number of scans T contributing to the innovation statistic. It follows by the change of variables

$\xi = \left(\kappa_m\lambda|R|^{\frac{1}{2}}\right)^{\frac{-2}{m}} \eta$ that

$$s_\alpha(\kappa_m\lambda|R|^{\frac{1}{2}}, T) = \left(\kappa_m\lambda|R|^{\frac{1}{2}}\right)^{\frac{-2}{m}} s_\alpha(T), \tag{16}$$

where the standardized threshold $s_\alpha(T)$ is defined by

$$1-\alpha = \int_{s_\alpha(T)}^{\infty} p_s(\eta \mid 1, T, \mathcal{H}')d\eta. \tag{17}$$

Computation of the standardized threshold $s_\alpha(T)$ is discussed in the appendix, where several tables are also given.

The initialization sensitivity region of significance α, denoted $\mathcal{R}'(\alpha)$, is defined by constraining the mean of the innovation statistic under $\mathcal{K}'$ to be less than or equal to the threshold $s_\alpha(\kappa_m\lambda|R|^{\frac{1}{2}}, T)$. The mean is the noncentrality parameter (equation (10)), so the region $\mathcal{R}'(\alpha)$ is given by the quadratic inequality

$$\mathcal{R}'(\alpha) \equiv \left\{ \Delta \in \boldsymbol{R}^n : \Delta' W \Delta \le \left(\kappa_m\lambda|R|^{\frac{1}{2}}\right)^{\frac{-2}{m}} s_\alpha(\mathrm{T}) \right\}, \tag{18}$$

where the identity (equation (16)) is substituted in equation (18). If W is positive definite, the significance region $\mathcal{R}'(\alpha)$ is a nondegenerate ellipsoid in the target state space, $\boldsymbol{R}^n$. If W is not positive definite, the significance region has infinite extent in directions corresponding to the eigenvectors of the zero eigenvalues of W. Track initialization in the significance region $\mathcal{R}'(\alpha)$ guarantees that the mean of $S_{\mathcal{K}'}$ does not exceed the significance level α, assuming PK track initialization. Intuitively, initializing in $\mathcal{R}'(\alpha)$ guarantees that at most α percent of all potential tracks generated by the NNAF in clutter are "track-like" in comparison with real tracks.

A more conservative initialization region is defined by specifying an additional significance level on the alternative hypothesis $\mathcal{K}'$. Let β denote the lower-tail significance level for the statistic $S_{\mathcal{K}'}$, that is, 1 - β is the probability of rejecting $\mathcal{K}'$. The initialization sensitivity region at the operating point (α,β), denoted $\mathcal{R}'(\alpha,\beta)$, is defined by

$$\mathcal{R}'(\alpha,\beta) \equiv \left\{ \Delta \in R^n : \int_{s_\alpha\left(\kappa_m \lambda |R|^{\frac{1}{2}}, T\right)}^{\infty} \chi^2_{mT}(\xi \mid \Delta' W \Delta)\, d\xi \le 1-\beta \right\}. \tag{19}$$

For every probability α there exists a probability β_0 such that

$$\mathcal{R}'(\alpha,\beta) \subseteq \mathcal{R}'(\alpha), \text{for all } \beta \le \beta_0,$$

that is, the initialization region $\mathcal{R}'(\alpha,\beta_0)$ is smaller than the region $\mathcal{R}'(\alpha)$ for all $\beta \le \beta_0$. A rough approximation is $\mathcal{R}'(\alpha) \approx \mathcal{R}'\left(\alpha,\frac{1}{2}\right)$.

The ROC curve for $\mathcal{H}'$ and $\mathcal{K}'$ is the locus of the point

$$\left(\int_0^s p_s(\xi \mid \lambda |R|^{\frac{1}{2}}, T, \mathcal{H}')\, d\xi,\ \int_0^s \chi^2_{mT}(\xi \mid \Delta W \Delta) d\xi \right), \tag{20}$$

as s ranges from zero to infinity. The integrals range over the interval (0, s) instead of the more typical interval (s,∞) because both hypothesis tests are lower-tail tests. The ROC curves (equation (20)) are functions of clutter density, initialization error, and T, so they are actually non-planar surfaces and, hence, difficult to visualize.

Insightful planar curves are obtained in the following manner: set the operating point (α,β) and, for every threshold s, define

$$\delta^*(s) = max\left\{ \delta : \beta \le \int_0^s \chi^2_{mT}(\xi \mid \delta) d\xi \right\}, \tag{21}$$

$$\lambda^*(s)\, |R|^{\frac{1}{2}} = max\left\{ \lambda |R|^{\frac{1}{2}} : \alpha \le \int_0^s p_s(\xi \mid \lambda |R|^{\frac{1}{2}}, T, \mathcal{H}') d\xi \right\}. \tag{22}$$

It can be verified that the equation defining the set in equation (21) has a unique solution for each $s \ge s(\beta)$, where $s(\beta)$ is the β percent point of the (central) chi-square distribution, i.e.,

$$\beta = \int_0^{s(\beta)} \chi^2_{mT}(\xi \mid 0) d\xi. \tag{23}$$

For $s \le s(\beta)$, the set in equation (21) is empty because no solution to the defining equation exists. The curve $(\sqrt{\delta^*(s)}, \lambda^*(s)|R|^{\frac{1}{2}})$ defined parametrically as s ranges from $s(\beta)$ to infinity is called the ICE curve, and it depends only on the number of scans T. ICE curves are useful in approximating the maximum density clutter in which targets can be successfully tracked. Knowledge of the sensor signal processor and clutter density determines target signal-to-noise ratio (SNR), so maximum clutter density estimates are equivalent to minimum target SNR estimates.

3. CRITICAL CLUTTER DENSITY

As discussed in section 2, critical clutter density occurs when the first moments of the statistics $S_{\mathcal{H}'}$ and $S_{\mathcal{K}'}$ are equal. Using the hypotheses $\mathcal{H}'$ and $\mathcal{K}'$ and equating the mean values of the statistics $S_{\mathcal{H}'}$ and $S_{\mathcal{K}'}$ gives

$$\overline{S_{\mathcal{H}'}} = T\bar{u} = mT + \delta = \overline{S_{\mathcal{K}'}} \tag{24}$$

Solving for the total squared initialization error δ gives the fundamental equation relating clutter density and track initialization error, namely,

$$\delta = T(\bar{u} - m) \equiv T\rho(\lambda) \ge 0, \tag{25}$$

where

$$\rho(\lambda) = \left[\frac{\Gamma\left(\frac{2}{m}+1\right)}{\pi} \left[\frac{\Gamma\left(\frac{m}{2}+1\right)}{\lambda |R|^{\frac{1}{2}}} \right]^{\frac{2}{m}} - m \right]. \tag{26}$$

The clutter density parameter λ appears only on the right-hand side of the equation. Solving the inequality $\rho(\lambda) \ge 0$ for λ gives

$$\lambda \le \lambda_{critical} = \frac{\Gamma\left(\frac{m}{2}+1\right)}{|R|^{\frac{1}{2}}} \left[\frac{\Gamma\left(\frac{2}{m}+1\right)}{\pi m} \right]^{\frac{m}{2}}. \tag{27}$$

The critical clutter density is a function only of the measurement dimension and the determinant of the covariance matrix of the additive Gaussian noise. The normalized critical clutter density, $\lambda_{critical}|R|^{\frac{1}{2}}$ depends only on the measurement dimension, a fact that is intuitively satisfying.

The critical clutter density is independent of the number of scans T, as might be anticipated from the problem formulation. More importantly, it also holds for general nonlinear target and measurement models. Different target and measurement process models (i.e., the functions $\{F_t\}$ and $\{H_t\}$) yield the same critical clutter density. This is not to say, however, that different models track equally well in the same density clutter.

The critical clutter density is defined via an extreme circumstance, namely when the means of two PDFs are equal. As such, the critical density should be interpreted as an upper bound at which a strictly kinematic tracking algorithm can be expected to operate. Such a performance limit provides a quantitative standard of comparison for alternative tracking algorithms in clutter. For example, a tracker that functions reliably at normalized clutter densities up to 10 percent of $\lambda_{critical}|R_{sensor\ 1}|^{\frac{1}{2}}$ is probably better than one that functions only up to 1 percent of $\lambda_{critical}|R_{sensor\ 2}|^{\frac{1}{2}}$. The utility of the normalized clutter density as a standard comparison measure deserves further examination in practical problems.

Particular values of the normalized critical density are, using equation (27),

$$\lambda_{critical}|R|^{\frac{1}{2}} = \frac{1}{\sqrt{2}},\ \frac{1}{2\pi},\ \frac{\sqrt{2}}{18\pi}\left[\Gamma\left(\frac{2}{3}\right)\right]^{\frac{3}{2}},\ \frac{1}{32\pi} \tag{28}$$

for measurement vector dimensions m = 1, 2, 3, and 4, respectively. Using Stirling's approximation to the Gamma function and the curious limit

$$\lim_{m\to\infty}\left\{\Gamma\left(1+\tfrac{1}{m}\right)\right\}^m = e^{-\gamma} \cong 0.561459, \tag{29}$$

where $\gamma \cong 0.577216$ is Euler's constant, gives the asymptotic result

$$\lambda_{critical}|R|^{\frac{1}{2}} = \frac{e^{-\gamma}\sqrt{m\pi}}{(2\pi e)^{\frac{m}{2}}},\ \text{as } m\to\infty. \tag{30}$$

It follows from equation (30) that

$$\lim_{m\to\infty} \frac{\lambda_{critical}\big|_m}{\lambda_{critical}\big|_{m+1}} = \sqrt{2\pi e} \cong 4.1327. \tag{31}$$

Evidently, the critical clutter density decreases with increasing measurement dimension m by a factor of about four for additional components of the measurement vector. As shown by the tabular data below, these limiting values are approached rather slowly.

m	$\lambda_{critical}\lvert R\rvert^{\frac{1}{2}}$	$\frac{\lambda_{critical}\big\lvert_m}{\lambda_{critical}\big\lvert_{m+1}}$	$\lambda_{critical}\lvert R\rvert^{\frac{1}{2}} \Big/ \frac{e^{-\gamma}\sqrt{m\pi}}{(2\pi e)^{\frac{m}{2}}}$
1	0.70711	4.4429	2.9365
2	0.15916	4.0387	1.9315
3	0.39407 (-1)	3.9617	1.6137
4	0.99472 (-2)	3.9472	1.4549
5	0.25201 (-2)	3.9504	1.3653
10	0.25589 (-5)	3.9965	1.1817
15	0.24660 (-8)	4.0287	1.1210
20	0.22981 (-11)	4.0492	1.0907
25	0.20958 (-14)	4.0631	1.0725
100	0.24098 (-60)	4.1130	1.0181
1000	0.18260 (-614)	4.1307	1.0018

4. EXAMPLE: CONSTANT VELOCITY TARGET

The example is uses a constant velocity target model with two dimensional measurements. For ease of exposition, measurement vector components are referred to as position coordinates. Measurement scans are available at fixed sampling intervals of $\tau > 0$. The units of time and position (e.g., seconds and meters) are irrelevant because standardized error coordinates (described below) are used throughout. Extension to constant acceleration target models is straightforward and not pursued in this report.

In the example $m = 2$, $n = 4$, and the constant velocity motion model is

$$F = \begin{bmatrix} 1 & \tau & 0 & 0 \\ 0 & 1 & 0 & 0 \\ 0 & 0 & 1 & \tau \\ 0 & 0 & 0 & 1 \end{bmatrix}, \; H = \begin{bmatrix} 1 & 0 & 0 & 0 \\ 0 & 0 & 1 & 0 \end{bmatrix}, \text{ and } R = \begin{bmatrix} \sigma^2 & 0 \\ 0 & \sigma^2 \end{bmatrix}. \tag{32}$$

The target state components are position x and velocity $\dot{x}$. From the definition (equation (14)), W is a 4×4 block diagonal matrix with the 2×2 diagonal blocks

$$W_d = \frac{1}{\sigma^2} \begin{bmatrix} T & \frac{1}{2}\tau T(T-1) \\ \frac{1}{2}\tau T(T-1) & \frac{1}{6}\tau^2 T(T-1)(2T-1) \end{bmatrix}. \tag{33}$$

W_d is singular for $\tau = 0$ because, in this case, the matrix F models a motionless target. For $\tau > 0$, the matrix W_d is singular for $T = 1$ because velocity is unobservable from a single position measurement. For the remainder of this section, it is assumed that $\tau > 0$ and $T \geq 2$. Let $(x, \dot{x}, y, \dot{y})$ denote the (transposed) target state vector. Standardized error coordinates for position and velocity are

$$\left(\frac{\Delta x}{\sigma}, \; \frac{\tau \Delta \dot{x}}{\sigma}, \; \frac{\Delta y}{\sigma}, \; \frac{\tau \Delta \dot{y}}{\sigma} \right),$$

where $(\Delta x, \Delta \dot{x}, \Delta y, \Delta \dot{y}) = (x_1^{\text{true}} - x_1^{\text{initial}}, \; \dot{x}_1^{\text{true}} - \dot{x}_1^{\text{initial}}, \; y_1^{\text{true}} - y_1^{\text{initial}}, \; \dot{y}_1^{\text{true}} - \dot{y}_1^{\text{initial}})$. The block structure of W and the explicit form (equation (33)) gives the initialization region

$$\mathcal{R}'(\alpha) \equiv \begin{pmatrix} \frac{\Delta x}{\sigma} \\ \frac{\Delta \dot{x}}{\sigma} \end{pmatrix}' W^{\circ} \begin{pmatrix} \frac{\Delta x}{\sigma} \\ \frac{\Delta \dot{x}}{\sigma} \end{pmatrix} + \begin{pmatrix} \frac{\Delta y}{\sigma} \\ \frac{\Delta \dot{y}}{\sigma} \end{pmatrix}' W^{\circ} \begin{pmatrix} \frac{\Delta y}{\sigma} \\ \frac{\Delta \dot{y}}{\sigma} \end{pmatrix}, \tag{34}$$

where the standardized matrix W° is defined by

$$W^{\circ} = \begin{bmatrix} T & \frac{1}{2}T(T-1) \\ \frac{1}{2}T(T-1) & \frac{1}{6}T(T-1)(2T-1) \end{bmatrix}.$$

Because the x and y coordinates separate in (34), the initialization region in this case is most easily studied by supposing no initialization error in one component. The eigenvalues of W° are

$$\begin{aligned} \gamma_{\pm} &= \frac{T}{2}\left[1+\tfrac{1}{6}(T-1)(2T-1) \pm \sqrt{\left(1+\tfrac{1}{6}(T-1)(2T-1)\right)^2 - \tfrac{1}{3}(T^2-1)}\right] \\ &= \frac{T}{2}\left[1+\tfrac{1}{6}(T-1)(2T-1) \pm \sqrt{1+\tfrac{1}{3}(T-1)(T-2)+\tfrac{1}{36}(T-1)^2(2T-1)^2}\right]. \end{aligned} \tag{35}$$

For $T \geq 2$, it is easily seen from these forms that the eigenvalues are distinct and positive. Consequently, W°, W_d ,and W are positive definite.

The positive branch of the square root in equation (35) gives the larger of the two eigenvalues. The lengths of the major and minor axes of the elliptical track initialization region $\mathcal{R}'$ in standardized error coordinates, are proportional to the square roots of the smallest and largest eigenvalues, respectively, of W°. Thus, the eccentricity of the ellipse is

$$eccentricity \equiv \frac{major\ axis\ length}{minor\ axis\ length} = \frac{\sqrt{\frac{1}{\gamma_-}}}{\sqrt{\frac{1}{\gamma_+}}} = \sqrt{\frac{\gamma_+}{\gamma_-}}.$$

For $T = 2$, 5, 10, 15, 20, and 25, the eccentricity rounded to the nearest integer is 3, 5, 10, 16, 22, and 27, respectively. Asymptotically,

$$\gamma_+ = \tfrac{1}{3}T^3 + o\left(T^2\right) \text{ and } \gamma_- = \tfrac{1}{4}T + o(1), \text{ as } T \to \infty, \tag{36}$$

so that

$$eccentricity = \sqrt{\tfrac{4}{3}}\ T + o(1), \text{ as } T \to \infty. \tag{37}$$

The initialization region eccentricity therefore increases linearly with T for large T.

The eigenvectors of W° corresponding to $\gamma_{\pm}$ are given by

$$e_{\pm} = \frac{1}{\sqrt{1+b_{\pm}^2}}\begin{pmatrix} 1 \\ b_{\pm} \end{pmatrix}, \tag{38}$$

where

$$b_{\pm} = \frac{1}{T-1}\left[-1+\tfrac{1}{6}(T-1)(2T-1) \pm \sqrt{1+\tfrac{1}{3}(T-1)(T-2)+\tfrac{1}{36}(T-1)^2(2T-1)^2}\right]. \tag{39}$$

The angle between the positive standardized position axis and the eigenvector e_- corresponding to major axis of W° is $\psi = tan^{-1}[b_-]$. For $T = 2$, 5, 10, 15, 20, and 25, ψ is -58°, -19°, -9°, -6°, -4°, and -3.5°, respectively. It is easily verified that $b_- < 0$ for $T \geq 2$, so ψ must be negative. Asymptotically,

$$\psi = \frac{-3}{2T} - o\left(\frac{1}{T^2}\right), \text{ as } T \to \infty. \tag{40}$$

For sufficiently large T, the angular "tilt" of the initialization region diminishes linearly with increasing T. The negative correlation between normalized position and velocity errors accords well with intuition.

The half-lengths L_+ and L_- of the major and minor axes, respectively, of the region are functions of clutter density and significance level α. Explicitly,

$$L_{\pm} = \frac{1}{\left(\kappa_m \lambda |R|^{\frac{1}{2}}\right)^{\frac{1}{m}}} \sqrt{\frac{s_\alpha(T)}{\gamma_{\mp}}}, \tag{41}$$

where the standardized threshold $s_\alpha(T)$ is tabulated in the appendix. From equation (28), the critical clutter density for two-dimensional measurements is $\frac{1}{2\pi}$, so a normalized clutter density representative of moderate to heavy clutter is

$$\lambda |R|^{\frac{1}{2}} \equiv \lambda\sigma^2 = \frac{10^{-1}}{2\pi}.$$

For $T = 2$, 5, 10, 15, 20, and 25 and for a 1-percent significance level (i.e., $\alpha = 0.01$), the major axis half-lengths are

$L_+ = 2.789$, 4.140, 5.409, 6.044, 6.434, and 6.704,

respectively; the minor axis half-lengths are

$L_- = 1.065$, 0.8737, 0.5317, 0.3818, 0.2986, and 0.2457,

respectively. These half-lengths assume no error in one component. For errors in both x and y

components, a more appropriate "average" initialization region is obtained by dividing these half-lengths by $\sqrt{2}$, assuming equal error contributions in each component.

Figure 1 shows the initialization region $\mathcal{R}'(\alpha)$ corresponding to 1-percent significance levels, respectively, for rejecting clutter for several choices of batch length T. The relative sizes of the major and minor axes of $\mathcal{R}'(\alpha)$, as well as the orientation angle ψ, agree with the results given above.

It is evident from figure 1 that, as T increases, track initialization error in standardized coordinates is more sensitive to initial velocity errors than to initial position errors. This trend confirms the asymptotic formulae given above. It follows that the allowable error in $\Delta\dot{x}$ (and in $\Delta\dot{y}$) is inversely proportional to the sample interval τ.

ICE curves are described in section 2 as a way to quantify the following intuitively reasonable statement: increasing the normalized clutter density requires progressively better track initialization to maintain a fixed significance level for rejecting clutter. However, ICE curves are not presented here.

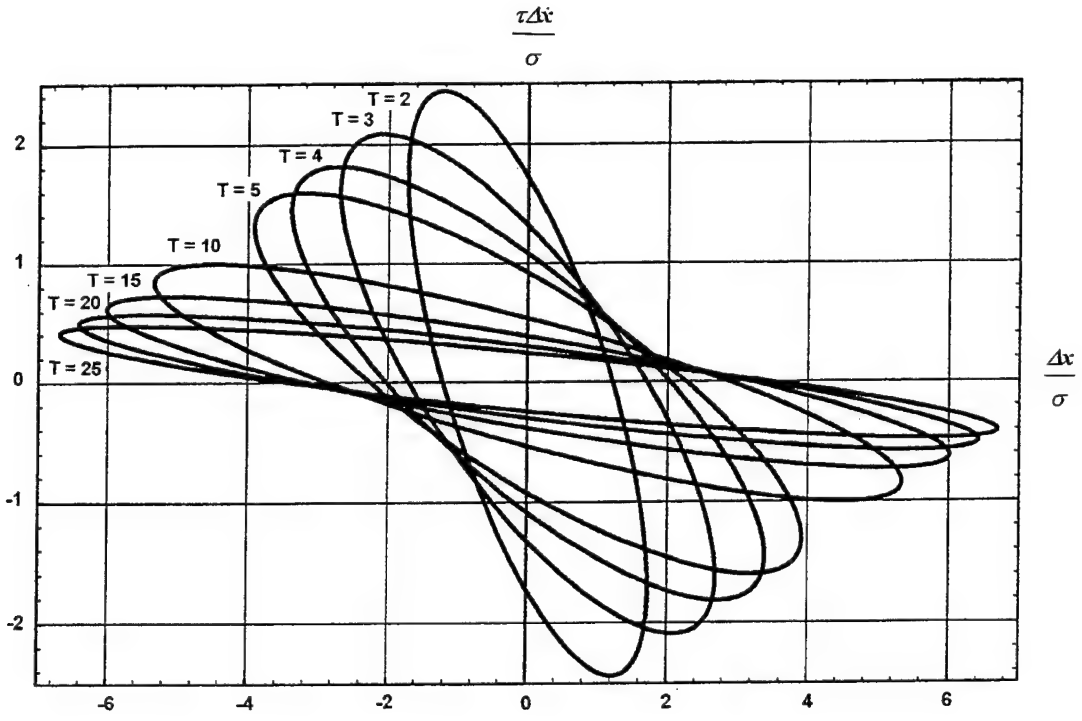

Figure 1. Initialization Error Regions for Significance Level $\alpha = 0.01$

5. CONCLUSIONS AND RECOMMENDATIONS

Further study of several topics is recommended. The utility of families of ICE curves as a means of quantifying the maximum clutter density in which target tracking can be reliably performed merits further study. The development of initialization error regions for constant acceleration target models also merits further study. The correct hypotheses $\mathcal{H}$ and $\mathcal{K}$ remain to be investigated. Finally, when non-kinematic information is exploited by the assignment function, the approach of this report is inadequate and must be reformulated. The best way to approach this topic depends on the application and the nature of the non-kinematic data used.

The approach developed is applicable to any filtering problem in which initialization in clutter is potentially a problem. The example presented suggests that this formulation provides a reasonable and useful method to assess the relative sensitivity of different state variables to initialization in clutter.

APPENDIX
COMPUTATION OF SIGNIFICANCE THRESHOLDS UNDER $\mathcal{H}'$

The standardized threshold $s_a(T)$ is defined by equations (16) and (17). For $m = 2$, it is easily shown that

$$p_s\left(\eta|1,\ T,\ \mathcal{H}'\right) = \frac{1}{(T-1)!}\eta^{T-1}\ e^{-\eta} \tag{A-1}$$

so that the cumulative function is, in this case, the incomplete Gamma function (see Abramowitz and Stegun, equation (6.5.1)).[6] Algorithms for computing the incomplete Gamma function are widely available (e.g., in *Mathematica*), so computing the threshold is simply a matter of solving the nonlinear equation (17). In *Mathematica*, Newton-Raphson's iteration for the solution is the following one line expression:

```
FindRoot[GammaRegularized[T,s]==1-alpha,{s,s0}],
```
(A-2)

where $s0$ is an initial guess at the solution, and *GammaRegularized*[ ] is an intrinsic *Mathematica* function that equals one minus the incomplete Gamma function. The algorithm (equation (A-2)) is insensitive to the choice of initial point $s0$.

For $m \neq 2$, the required PDF is not available in closed form, so computing the thresholds $s_\alpha(T)$ accurately requires numerically evaluating the characteristic function $f(\xi)$ of $p(u)$ and integrating $\left[f(\xi)\right]^T$. For full details, see Nuttall.[7] For the present purposes, however, approximate thresholds are easily computed by simulation using the following procedure. The exceedance of $p(u)$ for $\kappa_m \lambda |\boldsymbol{R}|^{\frac{1}{2}} = 1$ is, from equation (3),

$$E(v) = \int_v^\infty \frac{m}{2} u^{\frac{m}{2}-1}\ exp\left(-u^{\frac{m}{2}}\right) du = exp\left(-v^{\frac{m}{2}}\right). \tag{A-3}$$

Its inverse function is

$$v = \left(-ln\ E\right)^{\frac{2}{m}}. \tag{A-4}$$

Hence, if E is uniformly distributed on the interval (0,1), then v is distributed according to $p(u)$. Consequently, the sum

$$s = \sum_{t=1}^{T} v_t \tag{A-5}$$

is distributed $p_s(\cdot\,|1,T,\mathcal{H})$, provided each term v_i is computed via equation (A-4). Samples $\{s_n\}_{n=1}^{N}$ of the sum (equation (A-5)) are generated using equation (A-4) and a pseudo-random number generator and sorted so that $s_{(1)} \le s_{(2)} \le \cdots \le s_{(N)}$, where $s_{(n)}$ denotes the nth-order statistic. The lower-tail significance point $s_\alpha(T)$ is estimated as

$$s_\alpha(T) \approx s_{([\alpha N])}, \tag{A-6}$$

where $[\alpha N]$ in equation (A-6) denotes the greatest integer less than or equal to αN. Sample size N strongly affects the accuracy of the estimates (equation (A-6)), especially for small α. For sufficiently small values of α, the methods of reference 7 are recommended over simulation.

The tables below for $m \neq 2$ are compiled using $N = 10{,}000$ samples. These thresholds are probably accurate to about two digits. For $m = 2$, the numerical procedure described above is used to obtain thresholds that are rounded to the precision shown in tables A-1 and A-2.

Table A-1. Standardized Thresholds $s_\alpha(T)$ for m = 1 and m = 2.

	$m = 1$			$m = 2$ (exact)		
T	$\alpha = 0.1$	$\alpha = 0.01$	$\alpha = 0.001$	$\alpha = 0.1$	$\alpha = 0.01$	$\alpha = 0.001$
1	0.989(-2)	0.897(-4)	0.660(-6)	0.1054	0.1005(-1)	0.1001(-2)
2	0.190	0.130(-1)	0.154(-2)	0.5318	0.1486	0.4540(-1)
3	0.579	0.967(-1)	0.251(-1)	1.102	0.4360	0.1905
4	1.15	0.233	0.590(-1)	1.745	0.8232	0.4286
5	1.83	0.490	0.149	2.433	1.279	0.7394
6	2.60	0.906	0.374	3.152	1.785	1.107
7	3.58	1.27	0.505	3.895	2.330	1.520
8	4.50	1.69	0.702	4.656	2.906	1.971
9	5.50	2.15	1.08	5.432	3.507	2.452
10	6.46	2.85	1.56	6.221	4.130	2.961
15	12.3	3.83	3.83	10.30	7.477	5.794
20	18.8	6.96	6.96	14.53	11.08	8.958
25	25.8	10.7	10.7	18.84	14.85	12.34

Table A-2. Standardized Thresholds $s_\alpha(T)$ for m = 3 and m = 4

	$m = 3$			$m = 4$		
T	$\alpha = 0.1$	$\alpha = 0.01$	$\alpha = 0.001$	$\alpha = 0.1$	$\alpha = 0.01$	$\alpha = 0.001$
1	0.227	0.519(-1)	0.119(-1)	0.325	0.101	0.412(-1)
2	0.795	0.324	0.142	0.9758	0.505	0.248
3	1.459	0.763	0.463	1.64	1.04	0.689
4	2.12	1.20	0.802	2.37	1.60	1.14
5	2.81	1.81	1.25	3.16	2.27	1.73
6	3.56	2.40	1.88	3.87	2.90	2.32
7	4.35	3.05	2.35	4.64	3.54	2.87
8	5.07	3.77	2.84	5.46	4.21	3.46
9	5.81	4.35	3.35	6.20	4.99	4.05
10	6.61	4.99	4.04	7.01	5.73	4.72
15	10.6	8.60	7.27	11.1	9.31	8.15
20	14.7	12.1	10.8	15.5	13.2	11.9
25	18.7	15.8	14.1	19.2	16.9	15.6

REFERENCES

1. X. R. Li, "The PDF of Nearest Neighbor Measurement and a Probabilistic Nearest Neighbor Filter for Tracking in Clutter," *Proceedings of the 32nd IEEE Conference on Decision and Control*, San Antonio, TX, vol. 1, pp. 918-923, December 1993.

2. J. F. C. Kingman, *Poisson Processes*, Clarendon Press, Oxford, United Kingdom, 1993.

3. F. John, *Plane Waves and Spherical Means,* Springer-Verlag, New York, 1955.

4. P. G. Hoel, S. C. Port, and C. J. Stone, *Introduction to Probability Theory*, Houghton Mifflin, Boston, MA, 1971.

5. R. J. Muirhead, *Aspects of Multivariate Statistical Theory*, Wiley, New York, 1982.

6. M. Abramowitz and I. Stegun, *Handbook of Mathematical Functions*, National Bureau of Standards, Applied Mathematics Series 55, 10th Printing, 1972.

7. A. H. Nuttall, "Accurate Efficient Evaluation of Cumulative or Exceedance Probability Distributions Directly From Characteristic Functions," NUSC Technical Report 7023, Naval Underwater Systems Center, Newport, RI, 1 October 1983.

INITIAL DISTRIBUTION LIST

Addressee	No. of Copies
Program Executive Office for Cruise Missiles/Unmanned Aerial Vehicles	1
Program Executive Office for Undersea Warfare	1
Naval Research Laboratory	1
Naval Postgraduate School	1
Naval Surface Warfare Center	1
Naval Surface Warfare Center Coastal Systems Station, Panama City	1
Advanced Research Projects Agency	1
Defense Technical Information Center	12
Center for Naval Analyses	1